BAMS Article

Amplified Upward Trend of the Joint Occurrences of Heat and Ozone Extremes in China over 2013–20

Xiang Xiao, Yangyang Xu, Xiaorui Zhang, Fan Wang, Xiao Lu, Zongwei Cai, Guy Brasseur, and Meng Gao

ABSTRACT: Climate change and air pollution are two intimately interlinked global concerns. The frequency, intensity, and duration of heat waves are projected to increase globally under future climate change. A growing body of evidence indicates that health risks associated with the joint exposure to heat waves and air pollution can be greater than that due to individual factors. However, the cooccurrences of heat and air pollution extremes in China remain less explored in the observational records. Here we investigate the spatial pattern and temporal trend of frequency, intensity, and duration of cooccurrences of heat and air pollution extremes using China's nationwide observations of hourly $PM_{2.5}$ and O_3, and the ERA5 reanalysis dataset over 2013–20. We identify a significant increase in the frequency of cooccurrence of wet-bulb temperature (T_w) and O_3 exceedances (beyond a certain predefined threshold), mainly in the Beijing–Tianjin–Hebei (BTH) region (up by 4.7 days decade^{-1}) and the Yangtze River delta (YRD). In addition, we find that the increasing rate (compared to the average levels during the study period) of joint exceedance is larger than the rate of T_w and O_3 itself. For example, T_w and O_3 coextremes increased by 7.0% in BTH, higher than the percentage increase of each at 0.9% and 5.5%, respectively. We identify same amplification for YRD. This ongoing upward trend in the joint occurrence of heat and O_3 extremes should be recognized as an emerging environmental issue in China, given the potentially larger compounding impact to public health.

KEYWORDS: Air pollution; Ozone; Climate change

https://doi.org/10.1175/BAMS-D-21-0222.1

Corresponding author: Meng Gao, mmgao2@hkbu.edu.hk

Supplemental material: https://doi.org/10.1175/BAMS-D-21-0222.2

In final form 14 December 2021

AFFILIATIONS: Xiao, Zhang, and Wang—Department of Geography, Hong Kong Baptist University, Hong Kong, China; **Xu**—Department of Atmospheric Sciences, Texas A&M University, College Station, Texas; **Lu**—School of Atmospheric Sciences, Sun Yat-sen University, Guangzhou, China; **Cai**—State Key Laboratory of Environmental and Biological Analysis, Hong Kong Baptist University, Hong Kong, China; **Brasseur**—Atmospheric Chemistry Observation and Modeling Laboratory, National Center for Atmospheric Research, Boulder, Colorado; **Gao**—Department of Geography, and State Key Laboratory of Environmental and Biological Analysis, Hong Kong Baptist University, and Hong Kong Branch of Southern Marine Science and Engineering Guangdong Laboratory (Guangzhou), Hong Kong University of Science and Technology, Hong Kong, China

Global warming and ambient air pollution are two leading global public health concerns, driven by anthropogenic emissions of greenhouse gases and air pollutants from fossil fuel uses (IPCC 2014). It was estimated that the increase in global temperature would result in additional 250,000 deaths each year between 2030 and 2050 (Watts et al. 2015), while a recent assessment attributed 4.2 million premature deaths per year to ambient air pollution exposure (Cohen et al. 2017; WHO 2020). Climate change and air pollution are also intimately interlinked (Dean and Green 2018). A warming climate could directly alter meteorological variables, such as temperature, precipitation, and wind (Sanderson et al. 2011), and thus further affects physical and chemical processes of air pollution [e.g., ozone (O_3) and particulate matter ≤ 2.5 μm, ($PM_{2.5}$)] over multiple spatiotemporal scales (Ebi and McGregor 2008; Kinney 2008; Xu et al. 2018). Climate change is also likely to indirectly change particulate matter (PM) levels by modulating the natural emission from the occurrences of wildfires and dust storms (Dean and Green 2018).

Compared to the mean conditions of weather and air pollution, extreme weather and air pollution events, despite rare occurrences, can pose greater threats to human health and induce larger devastation to ecosystems and economy (IPCC 2012; Zhang et al. 2020). More concerning is that extreme air pollution episodes and heat waves often occur simultaneously because they can be driven by some common meteorological conditions. For example, heat waves, droughts, and peak ozone episodes are usually associated with stagnant high pressure systems (low precipitation, low wind speeds, sufficient solar radiation, etc.) that tend to accumulate heat and ozone precursors in a certain location. Moreover, complex interactions and feedbacks could happen to exacerbate extreme conditions. For example, high temperature during heat waves enhances biogenic emissions of volatile organic compounds (BVOCs) to increase production of O_3 and secondary organic aerosols (Karl et al. 2003). Under drought stress, stomatal uptake by plants is inhibited to reduce water loss, leading to a weaker dry deposition of O_3 and thus its higher surface concentrations (Gerosa et al. 2009; Lin et al. 2020).

Given that heat waves (Beniston 2004; Meehl and Tebaldi 2004; Stott et al. 2004; Fischer et al. 2007; Cowan et al. 2014; Schär 2016; Hoegh-Guldberg et al. 2018) and air pollution episodes (Mickley et al. 2004; Tagaris et al. 2007; Wu et al. 2008; Gao et al. 2017; Rieder et al. 2015; Schnell et al. 2016; Doherty et al. 2017; Schnell and Prather 2017) may aggravate over the coming decades, it is of great significance to analyze the historical trends of cooccurrence of heatwave and air pollution extremes, which would shed lights on the fidelity of their future projections. Another imperative to understand the cooccurrence of heatwave and air pollution extremes is driven by the recognitions that the simultaneous exposure to both air

pollution and heat wave may amplify the health consequences beyond the sum of individual effects (Basu 2009; Dear et al. 2010; Kan et al. 2012; Li et al. 2014; Ren et al. 2008; Stafoggia et al. 2008; Q. Wang et al. 2020; Willers et al. 2016; Zanobetti and Peters 2015).

Over the recent decade, air pollution, particularly the high $PM_{2.5}$ levels, have raised wide concerns in China (Gao et al. 2020a,b; Liang et al. 2017), and the State Council of China announced its strictest plan, the Air Pollution Prevention and Control Plan, in September 2013 (Zhang et al. 2019) to reduce the level of air pollutants. Since then, a decreasing trend of $PM_{2.5}$ levels have been found in both satellite and ground-level observations (Lin et al. 2018; Y. Wang et al. 2020; Wang et al. 2021). Despite of the overall decreasing trend, $PM_{2.5}$ concentrations during some pollution episodes can still exceed the threshold recommended by the World Health Organization (WHO) or local standards adopted in China (Y. Wang et al. 2020). Notably, while the concentrations of most primary pollutants have been decreasing in response to the emission control plan, surface O_3 concentrations have been increasing in several populated regions of China (Liu and Wang 2020; Lu et al. 2020; Y. Wang et al. 2020), and are projected to increase (Zhu and Liao 2016). Nevertheless, the variability and recent trend of the joint frequency of all three detrimental environmental stressors ($PM_{2.5}$, O_3, and heat extremes) have not been extensively explored in China. Here we present a series of spatiotemporal analyses based on various sources of observations from 2013 to 2020 ("Methods" section). The observationally based results here would be crucial to enhancing environmental protection measures and informing public health policies in the future (Chen et al. 2018; Xu et al. 2020).

Methods

Data sources of $PM_{2.5}$, O_3, and temperature. Nationwide observations of hourly $PM_{2.5}$ and O_3 concentrations from year 2013 to 2020 were obtained from the China National Environmental Monitoring Center (CNEMC) network. Starting from 2013 in 74 major cities, the CNEMC network now consists of more than 1,600 monitoring sites, covering 367 cities in China. $PM_{2.5}$ and O_3 were reported in units of micrograms per cubic meter ($\mu g\ m^{-3}$). Daily mean values of $PM_{2.5}$ were calculated from the hourly record. Daily maximum 8-h averages (MDA8) of O_3 were calculated as well. Hourly temperature and corresponding dewpoint temperature were taken from the ERA5 reanalysis dataset by the European Centre for Medium-Range Weather Forecasts (ECMWF) (Hersbach et al. 2020). Both temperature and dewpoint temperature from ERA5 were sampled at CNEMC sites to examine cooccurrences.

Definition of heat extremes using wet-bulb temperature. Previous studies suggested that a combination of temperature and humidity is a better metric to assess heat-related health risks (Kovats and Hajat 2008; Mora et al. 2017; Xu et al. 2020), as the human body is less able to cool itself efficiently by sweating under high humidity conditions. We adopted the wet-bulb temperature (T_w) in this study as the metric to define occurrences of heat waves (Sherwood 2018). The calculation of T_w assumes light wind speed and moderate radiation (Knutson and Ploshay 2016; Willett and Sherwood 2012), and thus only accounts for temperature (T) and humidity measures. In this study, we computed T_w using Stull's (2011) method:

$$T_w = T\ \mathrm{atan}\left[0.151977\left(100\times \mathrm{RH}+8.313659\right)^{1/2}\right]+\mathrm{atan}\left(T+100\times \mathrm{RH}\right)-\mathrm{atan}\left(100\times \mathrm{RH}-1.676331\right)$$
$$+0.00391838\left(100\times \mathrm{RH}\right)^{3/2}\times \tan\left(0.023101\times 100\times \mathrm{RH}\right)-4.686035, \quad (1)$$

where T_w denotes the wet-bulb temperature (°C), T the temperature (°C), RH the relative humidity. Because ERA5 provides dewpoint temperature only, RH was calculated by the following equation:

$$e_s = e_0 \times \exp\left[\frac{L_\upsilon}{R_w}\left(\frac{1}{T_0}-\frac{1}{T}\right)\right],\quad e_{\text{dew}} = e_0 \times \exp\left[\frac{L_\upsilon}{R_w}\left(\frac{1}{T_0}-\frac{1}{T_{\text{dew}}}\right)\right],\quad \text{RH} = \frac{e_{\text{dew}}}{e_s}\frac{p-e_s}{p-e_{\text{dew}}}\times 100\%, \tag{2}$$

where e_0 represents the reference water vapor pressure (611 Pa), and e_s and e_{dew} signify the water vapor pressure at saturation and at dewpoint temperature, respectively. The term T_0 refers to the reference temperature (273 K), T_{dew} denotes the dewpoint temperature, L_υ is the latent heat of water vaporization from liquid to gas (2.5×10^6 J kg^{-1}), and R_w represents the specific gas constant for water vapor (461.5 J kg^{-1} K^{-1}). Following Xu et al. (2020), we adopted daily average $T_w \geq 25$°C as the threshold for heat extremes.

Definition of air pollution extremes. We used the air quality standard of China (Zhao et al. 2016) for $PM_{2.5}$ and O_3, namely, 75 and 160 μg m^{-3}, as the cutoff values of exceedance. The days when daily mean T_w, daily mean $PM_{2.5}$, or MDA8 value for O_3 were higher than corresponding cutoff values were marked as exceedance days for each metric. The days when two or more metrics exceed thresholds simultaneously were further marked as cooccurring extreme days. The numbers of exceedance days were summarized by months for further trend analyses.

In addition to number of exceedance days (i.e., frequency of extreme events), we also considered the duration and severity of these extremes (Xu et al. 2020). Duration was defined as the number of successive days of extreme events. The severity was defined as the difference between the long-term average and the corresponding levels within the exceedance days only.

Statistical method for trend analyses. Previous studies have shown that heat waves and O_3 extremes often occur in warm seasons while $PM_{2.5}$ is typically more severe in cold seasons in China (Jia et al. 2017; Lu et al. 2020; Zheng et al. 2005), we therefore quantify the trend of T_w and O_3 during warm seasons only (six months from April to September), and for $PM_{2.5}$ we quantified the trend across the entire year. For the cooccurrence of T_w, O_3, and $PM_{2.5}$, we also used data during warm seasons. We assess the trends of monthly exceedance frequency (i.e., days per month) for heat waves, $PM_{2.5}$, and O_3 from 2013 to 2020, explicitly accounting for seasonal cycles and autocorrelation (Chandler and Scott 2011; Lu et al. 2020), as detailed below.

Trend analyses were performed by constructing a generalized linear regression equation with periodic functions accounting for seasonal variation and an autoregression term accounting for autocorrelation within the study period, as follows:

$$y_t = b + kt + \alpha\cos\left(\frac{2\pi M}{C}\right) + \beta\sin\left(\frac{2\pi M}{C}\right) + \text{AR}_t, \tag{3}$$

where y_t represents the exceedance frequency for the metrics of T_w, $PM_{2.5}$, and O_3 in month t, t denotes the index of month during the study period of 8 years (ranging from 1 to 48 for T_w and O_3, or from 1 to 96 for $PM_{2.5}$ alone), b denotes the intercept, k is the linear trend coefficient, α and β are coefficients of periodic functions, M is the month index in each year (ranging from 1 to 6 for T_w and O_3, or from 1 to 12 for $PM_{2.5}$ alone), C is the length of the seasonal cycle (6 for T_w and O_3, or 12 for $PM_{2.5}$ itself), and AR_t is the autoregression term for y_t. A nonparametric Mann–Kendall (M-K) test was performed to test the significance of linear trends.

Pooling to derive regional trend. Previous studies showed that the spatial distribution of O_3 concentrations vary greatly across different regions in China (Lu et al. 2018). Beijing–Tianjin–Hebei (BTH) region, Yangtze River delta (YRD) and Pearl River delta (PRD) region are three major urban clusters with distinct pollution patterns (Liu et al. 2018; Ma et al. 2019). In this study,

we calculated the aggregated/pooled trend of exceedances for T_w, O_3, and $PM_{2.5}$ as well as their joint occurrences in these three megacity clusters in China (BTH, YRD, and PRD).

However, the methods to generate regional trend in previous studies using observation data from monitoring sites seem arbitrary as each monitoring site may have depicted different and even opposite trends. A synthetical statistical algorithm is thus needed to standardize the calculation of regional trend. Here we propose a pooling method to aggregate the trends calculated from all individual sites within a specific region. The site-specific local trend, notated as k_i in the "Statistical method for trend analyses" section, are then pooled to estimate the average trend (K_r) representing a specific region following the equation of

$$K_r = \frac{\sum_{i=1}^{n} k_i w_i}{\sum_{i=1}^{n} w_i}, \tag{4}$$

where n is the number of sites within the region, and w_i is the weighting factor for each site i, defined as follows, similar to meta-analysis (Lipsey and Wilson 2001), where the standard error SE_i represents the uncertainty of estimating k_i

$$w_i = 1/\mathrm{SE}_i^2, \tag{5}$$

The average trend K_r is approximately normally distributed (Sánchez-Meca and Marín-Martínez 2010), and its sample variance could be defined as

$$\mathrm{Var}\left(K_r\right) = 1/\sum_{i=1}^{n} w_i, \tag{6}$$

Results and discussion

Spatiotemporal variations and long-term trend of T_w, O_3, and $PM_{2.5}$ exceedances. Humidity has critical effects on human body's reaction to temperature (Liu et al. 2014) as the human body is not able to cool itself by sweating under high humidity. Using temperature only may underestimate the severity of heat waves, especially in humid regions (Russo et al. 2017). In this study, we adopted 25°C as the threshold of heat extremes as proposed by Mora et al. (2017), and note that 25°C at a typical RH of 40% is very close to daily max temperature of 35°C (Xu et al. 2020). Over the southeastern coastal regions, T_w exceedance days could reach as high as 150–180 days annually (Fig. 1a and Fig. ES1 in the online supplement; https://doi.org/10.1175/BAMS-D-21-0222.2), suggesting high frequency of heat waves there. The average T_w in China displays a slightly increasing trend, rising from 13.5°C [standard deviation (SD): 5.6°C] in 2013 to 13.8°C (SD: 5.5°C) in 2020 (Fig. ES2). Moreover, the severity of high T_w extremes could reach up to 3°C (Fig. ES3) and the events (mean duration) could last about two months in southernmost part of China (Fig. ES4). Previously, Ding et al. (2010) and Wei and Chen (2011) reported a significant increase in heat waves across the nation during recent decades, except for a slight decrease in central China. In the shorter period of the last decade as examined here, however, the trend of T_w exceedance can go in both directions across China (Fig. 2). Overall, a clear positive trend could be found in mideastern and northeastern regions, on average, at rates of up to 1.4 days decade^{-1}. In

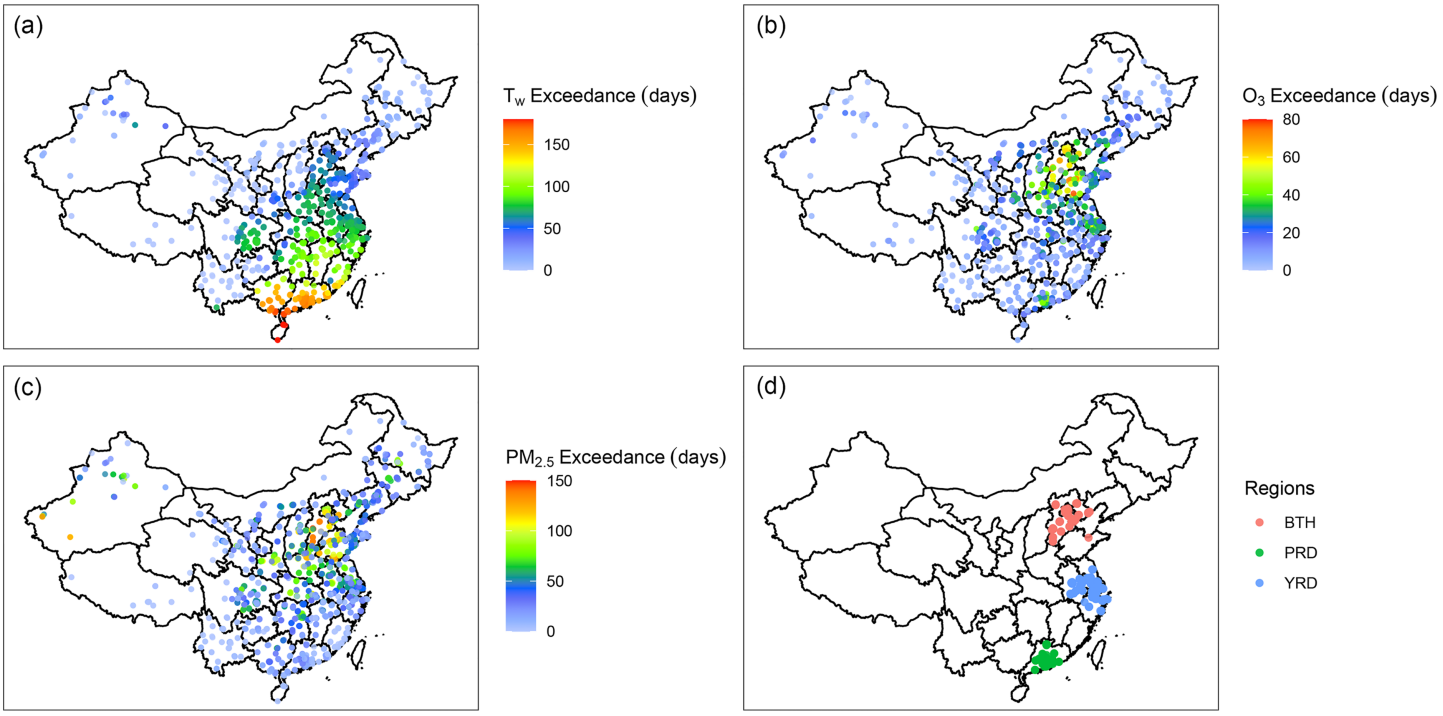

Fig. 1. Average number of exceedance days per year for (a) T_w, (b) O_3, and (c) $PM_{2.5}$; (d) locations of the sites in the BTH, PRD and YRD regions.

contrast, a decreasing trend, around 1.0 days decade^{-1} on average, is found in coastal and central areas of China.

Occurrences of O_3 exceedance were concentrated in the BTH, YRD, and PRD (locations marked in Fig. 1d), where intense human activities are located (Fig. 1b). Exceedance days exhibited a general increase over 2013–20 (up to 6.0 days decade^{-1}, Fig. 2b), in line with the variations of O_3 levels (Figs. ES5 and ES6). Despite extremely high levels of MDA8 O_3 (i.e., >30 μg m^{-3} above the threshold value) becoming less frequent, a modest exceedance (approximately 15–30 μg m^{-3} above the threshold values) was observed in more sites in recent years (Fig. ES7). The increase in the mean duration of O_3 extremes (Fig. ES8) also highlighted the nationwide spread of O_3 pollution, among which BTH area showed the most significant growth, consistent with previous studies (G. Li et al. 2017). The BTH is severely polluted with respect to $PM_{2.5}$, and mean exceedance days generally reached over 60 days (Fig. 1c). The number of exceedances of $PM_{2.5}$ reached a daunting 150 days per year in 2013–16 (Fig. ES9), which improved gradually since 2015 (He et al. 2020; Y. Wang et al. 2020; Xue et al. 2020), with both lower $PM_{2.5}$ levels (Fig. ES10) and lower severity observed (Fig. ES11). $PM_{2.5}$ exceedance days decreased at the rate of more than 10 days decade^{-1}, with the largest decreasing trend observed in BTH area (Fig. 2c).

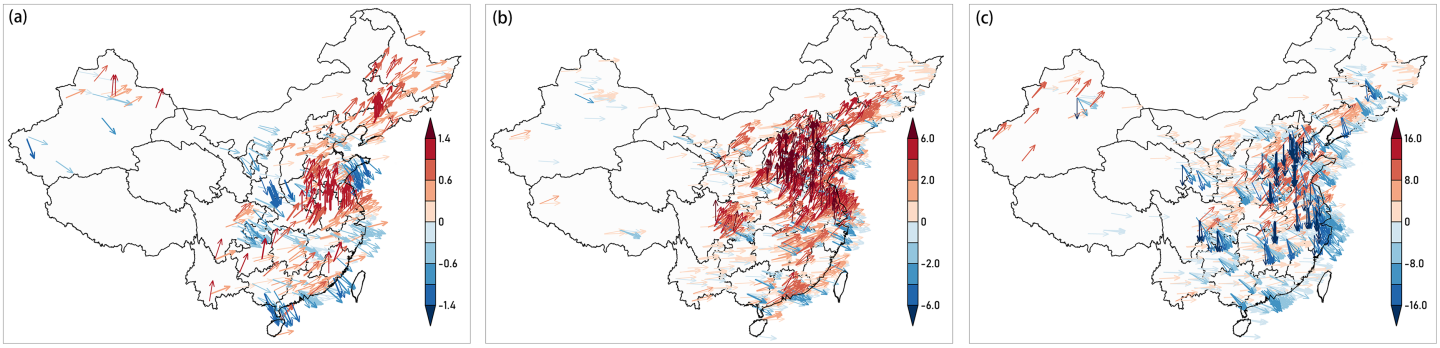

Fig. 2. Trend of (a) T_w, (b) O_3, and (c) $PM_{2.5}$ exceedance days. Both the angle and color are showing the negative trends (i.e., downward sloping arrows in blue color) and positive trends (i.e., upward sloping arrows in red color).

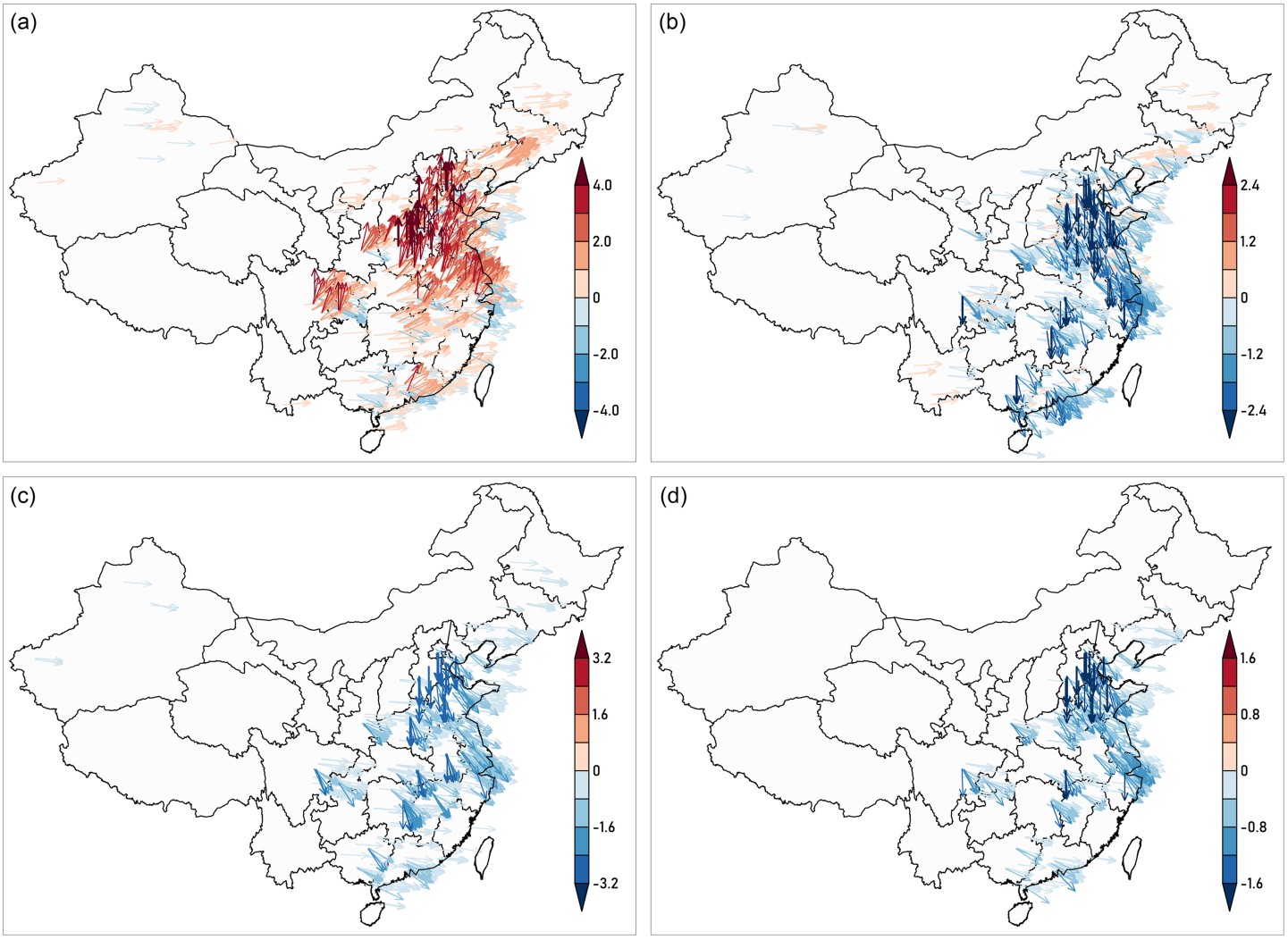

Fig. 3. Trend of cooccurrence of T_w, O_3, and $PM_{2.5}$ exceedance days over China. Cooccurrence of (a) T_w and O_3, (b) $PM_{2.5}$ and O_3, (c) T_w and $PM_{2.5}$, T_w, and (d) $PM_{2.5}$ and O_3. Both the angle and color are showing the negative trends (i.e., downward sloping arrows in blue color) and positive trends (i.e., upward sloping arrows in red color).

Changes in the joint exceedance of T_w, O_3, and $PM_{2.5}$. Figure 3 displays the trends of joint exceedance frequency of T_w, O_3, and $PM_{2.5}$ over the 2013–20 period. Here, we identify an alarming trend of cooccurrence of T_w and O_3 extremes. High T_w and O_3 extremes tend to increase in the study period, especially in the BTH and YRD regions (at a rate up to 4.0 days decade^{-1}). Among exceedance days, mean duration and severity of T_w and O_3 cooccurrence, we observe similar spatiotemporal pattern, in which the rising trend of T_w and O_3 is larger individually than jointly (absolute changes, Figs. ES13 and ES14), and most of the upward trend is observed in BTH and YRD regions driven by the cooccurrence in midsummer (June and July, figures not shown).

The cooccurrence of O_3 extremes during heat waves has long been recognized in developed countries (Filleul et al. 2006; Lee et al. 2006), and the underlying reason behind the combination of the two risk factors may partially be their common favorable weather patterns. For example, atmospheric blocking was reported to enhance the probability of cooccurrences of O_3 and heat extremes (Otero et al. 2022). Under a warming climate, amplified atmospheric blocking events are likely to lead to more frequent joint occurrences of heat and O_3 extremes (Nabizadeh et al. 2019). During heat waves, the stagnant condition, controlled by an anticyclone with a sinking airflow, may lead to less cloud cover (Pu et al. 2017) and weaker surface winds (K. Li et al. 2017), both of which are favorable for O_3 formation (Pyrgou et al. 2018).

Table 1. Average trends in percentage per decade (calculated with respect to the mean levels of each metric over the study period).

	Exceedance days			Mean duration		
Percentage change	All	BTH	YRD	All	BTH	YRD
T_w	1.0%	0.9%	0.8%	9.1%	–59.4%	4.8%
O_3	8.2%	5.5%	6.6%	142.6%	92.1%	142.5%
$PM_{2.5}$	–3.8%	–12.0%	–10.9%	–28.2%	–82.9%	–97.1%
T_w and O_3	10.9%	7.0%	7.5%	112.2%	68.9%	139.0%
T_w and $PM_{2.5}$	–29.0%	–26.5%	–33.3%	–174.0%	–170.7%	305.4%
O_3 and $PM_{2.5}$	–28.6%	–21.1%	–33.9%	–86.0%	–183.5%	–148.8%
T_w, O_3, and $PM_{2.5}$	–24.8%	–22.2%	–28.5%	–127.0%	–142.3%	–190.3%

Besides, previous review has indicated that high temperatures could play a catalytic role in promoting chemical reactions of O_3 formation and enhancing natural emissions of O_3 precursors; temperature is also associated with other synoptic patterns such as blocks and stagnation (Lu et al. 2019; Wang et al. 2017).

In addition, as important O_3 precursors, changes in anthropogenic emissions of NO_x, CO, and volatile organic compounds (VOCs) could also play a role in the observed patterns (Logan 1985; Lu et al. 2018; Qu et al. 2014). Previous numerical experiments suggested that NO_x reductions and aerosol control measures were the major cause for enhanced O_3 in Beijing, while reductions of NO_x and increase in VOCs emissions contributed to O_3 increase in Shanghai (Liu and Wang 2020). Accordingly, effective strategies of VOCs emission control should be also considered in high priority (He et al. 2022).

The cooccurrence of T_w, $PM_{2.5}$, and O_3 exceedance days had been decreasing at majority of sites, among which the greatest decreasing trend was observed in BTH (Fig. 3d). The trend of duration of these coextremes also showed a similar pattern (Fig. ES14). We observe that although $PM_{2.5}$ increased at a small number of sites (Fig. 2c), the joint occurrence of $PM_{2.5}$ and O_3 is found to decrease at nearly all sites (Fig. 3b). This is possibly associated with the fact that elevated $PM_{2.5}$ levels would reduce O_3 levels due to aerosols' influences on O_3 photochemistry and heterogeneous chemistry (Chen et al. 2020; Li et al. 2019).

In addition to the augmented cases (absolute changes) of cooccurrence of T_w and O_3, we ascertain in this study that the cooccurrence of T_w and O_3 have been increasing at higher percentage rates than the individual pace of each. As shown in Table 1, the exceedance days of T_w, and O_3 increased by 1.0% and 8.2% decade^{-1}, respectively, while the joint exceedance of T_w and O_3 showed an augmented increase by 10.8% decade^{-1}. Such an enhancement in the joint occurrences might be due to the abovementioned interaction between temperature and O_3 formation. Additionally, these numbers also indicate that although the cooccurrence of T_w and O_3 extremes was relatively rare in most cities, they have become more common in the recent years at a disproportionately larger rate.

Regional trend in BTH, YRD, and PRD. Among the three regions, BTH showed the highest downward trend (–13.0 days decade^{-1}) in $PM_{2.5}$ exceedances, followed by YRD (–7.7 days decade^{-1}) and PRD (–4.6 days decade^{-1}) (Fig. ES15). Opposite trends were identified for O_3 exceedances, with BTH increasing at 11.4 days decade^{-1}, YRD increasing at 5.5 days decade^{-1}, and PRD increasing at 1.7 days decade^{-1}. The exceedance trends of T_w were also positive, despite with a relatively smaller magnitude (0.9 days decade^{-1} for BTH, 3.8 days decade^{-1} for YRD, and 4.3 days decade^{-1} for PRD) (Fig. ES15).

Since the cooccurrences of T_w, O_3, and $PM_{2.5}$ were relatively rare in the PRD region, next we only report results for the BTH and YRD. In the BTH, the cooccurrence of T_w and O_3 increased at 4.7 days decade^{-1} (or relatively at 7.0% decade^{-1}) while all other combinations

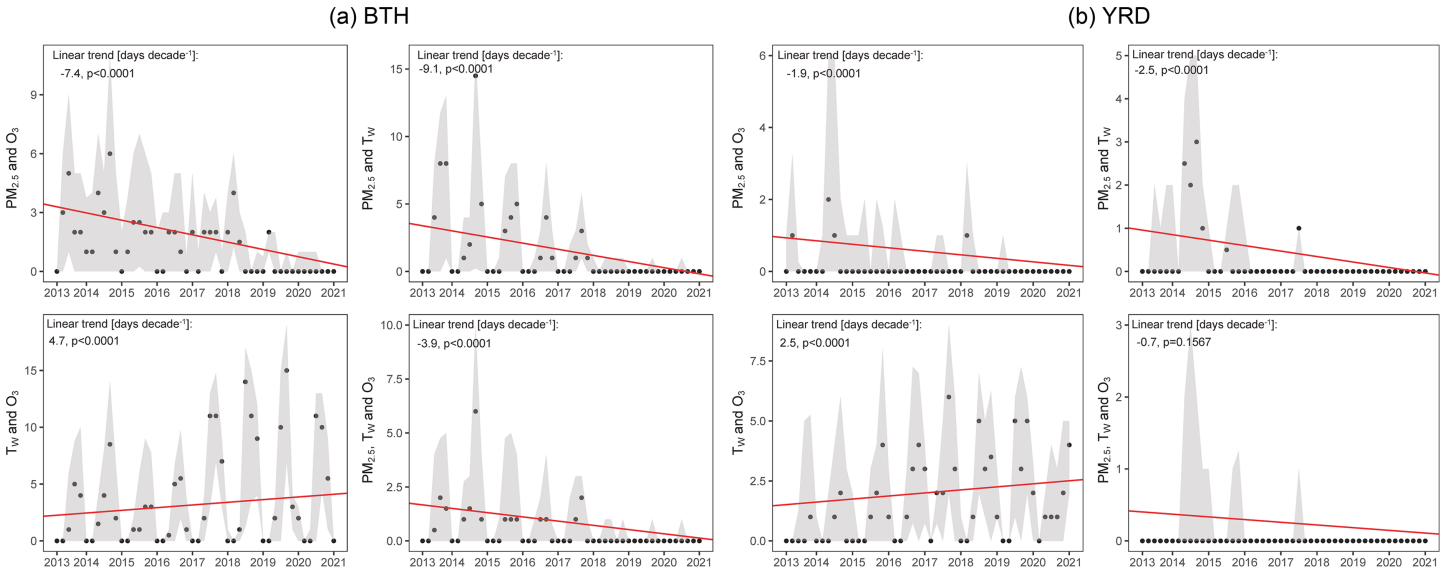

Fig. 4. Pooling trends of cooccurrence of T_w, O_3, and $PM_{2.5}$ exceedance days in the (a) BTH and (b) YRD regions.

exhibited decreasing trends (Figs. 4 and 5a). Similar patterns are found in the YRD (Figs. 4 and 5b). Similarly, increasing trends of T_w and O_3 severity and extreme duration were also identified in these two regions (Figs. ES16 and ES17). In BTH, we observe also that the exceedance days of T_w and O_3 coextremes increased by 7.0%, higher than the percentage of each of them (0.9% and 5.5%, respectively, Table 1). Same amplification is also identified for the YRD.

Interpretation of the amplified trends. As there is no census on the definition of heat waves around the globe. Previous studies that adopted various definitions of heat waves have revealed differences of effect estimation under different definitions (Chen et al. 2015; Kent et al. 2014). Our study found that absolute changes in the rising trend of T_w and O_3 is larger individually than jointly while the percentage rates showed the opposite pattern. This counterintuitive result may be partially due to the small number of cooccurrence as we used the mean values of each metrics to derive the percentage change. In addition, the uncertainty

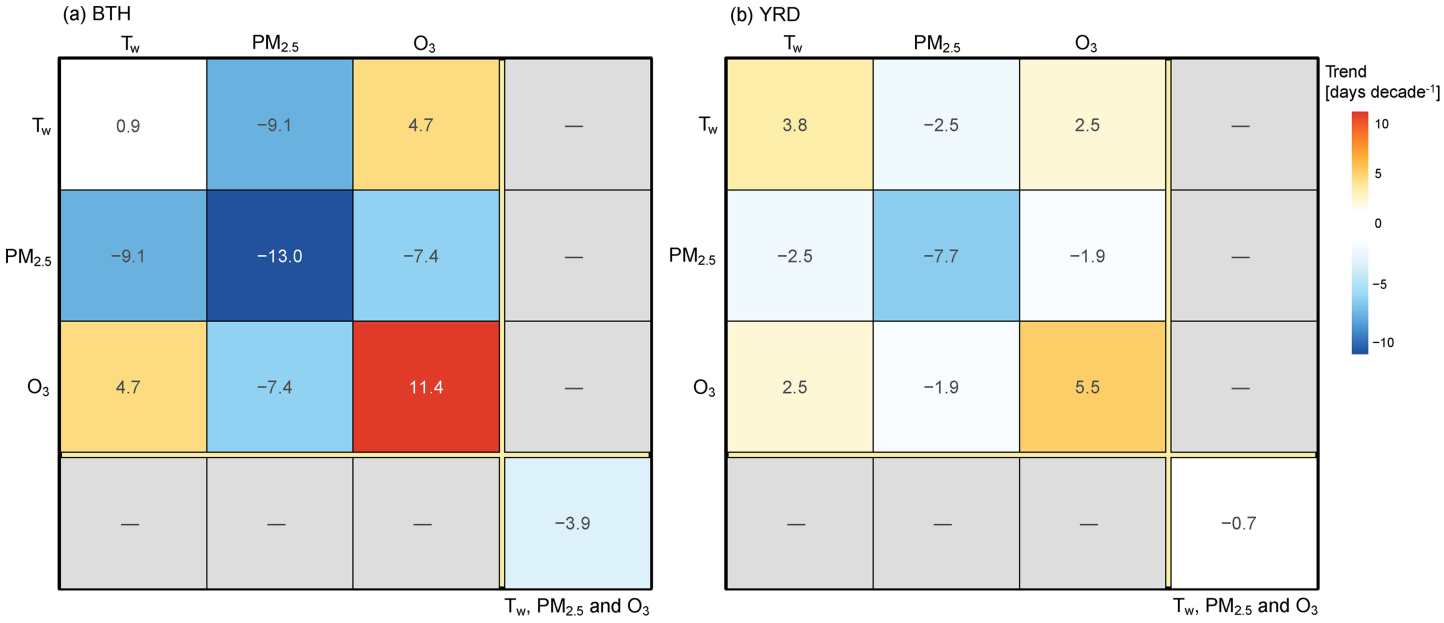

Fig. 5. Pooling trend of independent and joint occurrence of T_w, O_3, and $PM_{2.5}$ exceedance days in (a) BTH and (b) YRD.

of percentage change might also exist when using other definitions of heat wave. But our sensitivity analysis (Figs. ES21 and ES22) revealed that the direction and significance remain robust when using different threshold values. The amplified trend of T_w and O_3 we observed might be associated with multifactors, such as urban growth, anthropogenic heat, and $PM_{2.5}$ reduction. In addition, heatwave trends were also suggested to be associated with the local hydroclimate (Liao et al. 2018). Further investigations are needed to understand the contributions of different factors to the observed amplified trend of T_w and O_3. Another limitation of this study is that we used the fixed-effect model to obtain the average trend estimates in specific regions. The fixed-effect model made an assumption that the weight of the trend at each site is simply determined by the corresponding variance residuals (lower indicating better model performance) of trend regression model. Other factors such as geographical and meteorological conditions (such as elevation and wind speed) of each site cannot be considered.

Conclusions

In the trend pooling analyses, we used a strategy to assess the overall trend of a particular region. The results are not sensitive to outliers in the time series of data. We first followed the trend analyses method proposed and used in previous studies (Chandler and Scott 2011; Cochrane and Orcutt 1949; Weatherhead et al. 1998), and then we combined the trend within regions by using a standard error-based weighting method. The results are consistent with previous studies. For example, contrasting trends of $PM_{2.5}$ and surface O_3 concentrations were observed among all of the three regions (Y. Wang et al. 2020). In addition, we also found that the severity of ozone pollution (difference between mean concentration and its threshold value) was also on the rise.

BTH, YRD, and PRD are the three major city clusters in China and several studies have indicated that, in urban areas of these region, ozone formation is mainly VOC limited or mixed limited (Geng et al. 2009; Qu et al. 2014; Shao et al. 2009). For mixed-limited regions, it has been suggested that both decreasing NO_x levels and increasing VOCs levels could enhance ozone pollution (Lu et al. 2018). Furthermore, dealing with warming temperature and ozone pollution may have some cobenefits due to the relationship between temperature and ozone formation as discussed above as well as the fact that tropospheric ozone is a potent greenhouse gas. Therefore, cooperation in policies regarding warming climate and urban ozone pollution is warranted and further studies are needed to quantify the effect of emission control measures on both climate change and air pollution.

We conclude that China has achieved success in mitigating particulate matter pollution, as reduction in average concentration level, and in the frequency, duration, and severity of exceedance events have been observed. However, widespread ozone pollution and warming temperatures as well as the less-recognized cooccurrence of these two conditions are on the rise across the country. These two damaging factors for public health and ecosystems (Chen et al. 2007; Rossati 2017) should be seen as an emerging alarming issue. Further investigation on both aspects is needed to develop control strategies that effectively mitigate the ongoing trend and avoid undesired consequences.

Acknowledgments. We acknowledge the European Centre for Medium-Range Weather Forecasts (ECWMF) for providing the ERA5 reanalysis datasets. This study was supported by grants from Research Grants Council of the Hong Kong Special Administrative Region, China (Project HKBU22201820 and HKBU12202021), National Natural Science Foundation of China (42005084), and Natural Science Foundation of Guangdong Province (2019A1515011633).

Data availability statement. All the data presented can be accessed through contacting the corresponding authors.

References

Basu, R., 2009: High ambient temperature and mortality: A review of epidemiologic studies from 2001 to 2008. *Environ. Health*, **8**, 40, https://doi.org/10.1186/1476-069X-8-40.

Beniston, M., 2004: The 2003 heat wave in Europe: A shape of things to come? An analysis based on Swiss climatological data and model simulations. *Geophys. Res. Lett.*, **31**, L02202, https://doi.org/10.1029/2003GL018857.

Chandler, R., and M. Scott, 2011: *Statistical Methods for Trend Detection and Analysis in the Environmental Sciences.* John Wiley and Sons, 392 pp.

Chen, K., J. Bi, J. Chen, X. Chen, L. Huang, and L. Zhou, 2015: Influence of heat wave definitions to the added effect of heat waves on daily mortality in Nanjing, China. *Sci. Total Environ.*, **506–507**, 18–25, https://doi.org/10.1016/j.scitotenv.2014.10.092.

——, and Coauthors, 2018: Future ozone-related acute excess mortality under climate and population change scenarios in China: A modeling study. *PLOS Med.*, **15**, e1002598, https://doi.org/10.1371/journal.pmed.1002598.

Chen, S., H. Wang, K. Lu, L. Zeng, M. Hu, and Y. Zhang, 2020: The trend of surface ozone in Beijing from 2013 to 2019: Indications of the persisting strong atmospheric oxidation capacity. *Atmos. Environ.*, **242**, 117801, https://doi.org/10.1016/j.atmosenv.2020.117801.

Chen, T.-M., W. G. Kuschner, J. Gokhale, and S. Shofer, 2007: Outdoor air pollution: Ozone health effects. *Amer. J. Med. Sci.*, **333**, 244–248, https://doi.org/10.1097/MAJ.0b013e31803b8e8c.

Cochrane, D., and G. H. Orcutt, 1949: Application of least squares regression to relationships containing auto-correlated error terms. *J. Amer. Stat. Assoc.*, **44**, 32–61.

Cohen, A. J., and Coauthors, 2017: Estimates and 25-year trends of the global burden of disease attributable to ambient air pollution: An analysis of data from the Global Burden of Diseases Study 2015. *Lancet*, **389**, 1907–1918, https://doi.org/10.1016/S0140-6736(17)30505-6.

Cowan, T., A. Purich, S. Perkins, A. Pezza, G. Boschat, and K. Sadler, 2014: More frequent, longer, and hotter heat waves for Australia in the twenty-first century. *J. Climate*, **27**, 5851–5871, https://doi.org/10.1175/JCLI-D-14-00092.1.

Dean, A., and D. Green, 2018: Climate change, air pollution and human health in Sydney, Australia: A review of the literature. *Environ. Res. Lett.*, **13**, 053003, https://doi.org/10.1088/1748-9326/aac02a.

Dear, K., G. Ranmuthugala, T. Kjellström, C. Skinner, and I. Hanigan, 2010: Effects of temperature and ozone on daily mortality during the August 2003 heat wave in France. *Arch. Environ. Occup. Health*, **60**, 205–212, https://doi.org/10.3200/AEOH.60.4.205-212.

Ding, T., W. Qian, and Z. Yan, 2010: Changes in hot days and heat waves in China during 1961–2007. *Int. J. Climatol.*, **30**, 1452–1462, https://doi.org/10.1002/joc.1989.

Doherty, R. M., M. R. Heal, and F. M. O'Connor, 2017: Climate change impacts on human health over Europe through its effect on air quality. *Environ. Health*, **16**, 33–44, https://doi.org/10.1186/s12940-017-0325-2.

Ebi, K. L., and G. McGregor, 2008: Climate change, tropospheric ozone and particulate matter, and health impacts. *Environ. Health Perspect.*, **116**, 1449–1455, https://doi.org/10.1289/ehp.11463.

Filleul, L., and Coauthors, 2006: The relation between temperature, ozone, and mortality in nine French cities during the heat wave of 2003. *Environ. Health Perspect.*, **114**, 1344–1347, https://doi.org/10.1289/ehp.8328.

Fischer, E. M., S. I. Seneviratne, P. L. Vidale, D. Lüthi, and C. Schär, 2007: Soil moisture–atmosphere interactions during the 2003 European summer heat wave. *J. Climate*, **20**, 5081–5099, https://doi.org/10.1175/JCLI4288.1.

Gao, M., and Coauthors, 2020a: China's emission control strategies have suppressed unfavorable influences of climate on wintertime $PM_{2.5}$ concentrations in Beijing since 2002. *Atmos. Chem. Phys.*, **20**, 1497–1505, https://doi.org/10.5194/acp-20-1497-2020.

——, and Coauthors, 2020b: Ozone pollution over China and India: Seasonality and sources. *Atmos. Chem. Phys.*, **20**, 4399–4414, https://doi.org/10.5194/acp-20-4399-2020.

Gao, W., X. Tie, J. Xu, R. Huang, X. Mao, G. Zhou, and L. Chang, 2017: Long-term trend of O_3 in a mega City (Shanghai), China: Characteristics, causes, and interactions with precursors. *Sci. Total Environ.*, **603–604**, 425–433, https://doi.org/10.1016/j.scitotenv.2017.06.099.

Geng, F., and Coauthors, 2009: Aircraft measurements of O_3, NO_x, CO, VOCs, and SO_2 in the Yangtze River delta region. *Atmos. Environ.*, **43**, 584–593, https://doi.org/10.1016/j.atmosenv.2008.10.021.

Gerosa, G., A. Finco, S. Mereu, M. Vitale, F. Manes, and A. B. Denti, 2009: Comparison of seasonal variations of ozone exposure and fluxes in a Mediterranean Holm oak forest between the exceptionally dry 2003 and the following year. *Environ. Pollut.*, **157**, 1737–1744, https://doi.org/10.1016/j.envpol.2007.11.025.

He, Q., Y. Gu, and M. Zhang, 2020: Spatiotemporal trends of $PM_{2.5}$ concentrations in central China from 2003 to 2018 based on MAIAC-derived high-resolution data. *Environ. Int.*, **137**, 105536, https://doi.org/10.1016/j.envint.2020.105536.

He, Z., P. Liu, X. Zhao, X. He, J. Liu, and Y. Mu, 2022: Responses of surface O_3 and $PM_{2.5}$ trends to changes of anthropogenic emissions in summer over Beijing during 2014–2019: A study based on multiple linear regression and WRF-Chem. *Sci. Total Environ.*, **807**, 150792, https://doi.org/10.1016/j.scitotenv.2021.150792.

Hersbach, H., and Coauthors, 2020: The ERA5 global reanalysis. *Quart. J. Roy. Meteor. Soc.*, **146**, 1999–2049, https://doi.org/10.1002/qj.3803.

Hoegh-Guldberg, O., and Coauthors, 2018: Impacts of 1.5°C global warming on natural and human systems. *Global Warming of 1.5°C*, IPCC, 175–311.

IPCC, 2012: *Managing the Risks of Extreme Events and Disasters to Advance Climate Change Adaptation.* C. B. Field et al., Eds., Cambridge University Press, 582 pp.

——, 2014: *Climate Change 2014: Synthesis Report*. IPCC, 151 pp.

Jia, M., and Coauthors, 2017: Inverse relations of $PM_{2.5}$ and O_3 in air compound pollution between cold and hot seasons over an urban area of east China. *Atmosphere*, **8**, 59, https://doi.org/10.3390/atmos8030059.

Kan, H., R. Chen, and S. Tong, 2012: Ambient air pollution, climate change, and population health in China. *Environ. Int.*, **42**, 10–19, https://doi.org/10.1016/j.envint.2011.03.003.

Karl, T., A. Guenther, C. Spirig, A. Hansel, and R. Fall, 2003: Seasonal variation of biogenic VOC emissions above a mixed hardwood forest in northern Michigan. *Geophys. Res. Lett.*, **30**, 2186, https://doi.org/10.1029/2003GL018432.

Kent, S. T., L. A. McClure, B. F. Zaitchik, T. T. Smith, and J. M. Gohlke, 2014: Heat waves and health outcomes in Alabama (USA): The importance of heat wave definition. *Environ. Health Perspect.*, **122**, 151–158, https://doi.org/10.1289/ehp.1307262.

Kinney, P. L., 2008: Climate change, air quality, and human health. *Amer. J. Prev. Med.*, **35**, 459–467, https://doi.org/10.1016/j.amepre.2008.08.025.

Knutson, T. R., and J. J. Ploshay, 2016: Detection of anthropogenic influence on a summertime heat stress index. *Climatic Change*, **138**, 25–39, https://doi.org/10.1007/s10584-016-1708-z.

Kovats, R. S., and S. Hajat, 2008: Heat stress and public health: A critical review. *Annu. Rev. Public Health*, **29**, 41–55, https://doi.org/10.1146/annurev.publhealth.29.020907.090843.

Lee, J. D., and Coauthors, 2006: Ozone photochemistry and elevated isoprene during the UK heatwave of August 2003. *Atmos. Environ.*, **40**, 7598–7613, https://doi.org/10.1016/j.atmosenv.2006.06.057.

Li, G., L. Jiang, Y. Zhang, Y. Cai, X. Pan, and M. Zhou, 2014: The impact of ambient particle pollution during extreme-temperature days in Guangzhou City, China. *Asia Pac. J. Public Health*, **26**, 614–621, https://doi.org/10.1177/1010539514529811.

——, and Coauthors, 2017: Widespread and persistent ozone pollution in eastern China during the non-winter season of 2015: Observations and source attributions. *Atmos. Chem. Phys.*, **17**, 2759–2774, https://doi.org/10.5194/acp-17-2759-2017.

Li, K., and Coauthors, 2017: Meteorological and chemical impacts on ozone formation: A case study in Hangzhou, China. *Atmos. Res.*, **196**, 40–52, https://doi.org/10.1016/j.atmosres.2017.06.003.

——, D. J. Jacob, H. Liao, L. Shen, Q. Zhang, and K. H. Bates, 2019: Anthropogenic drivers of 2013–2017 trends in summer surface ozone in China. *Proc. Natl. Acad. Sci. USA*, **116**, 422–427, https://doi.org/10.1073/pnas.1812168116.

Liang, F., M. Gao, Q. Xiao, G. R. Carmichael, X. Pan, and Y. Liu, 2017: Evaluation of a data fusion approach to estimate daily $PM_{2.5}$ levels in North China. *Environ. Res.*, **158**, 54–60, https://doi.org/10.1016/j.envres.2017.06.001.

Liao, W., and Coauthors, 2018: Stronger contributions of urbanization to heat wave trends in wet climates. *Geophys. Res. Lett.*, **45**, 11 310–11 317, https://doi.org/10.1029/2018GL079679.

Lin, C. Q., G. Liu, A. K. H. Lau, Y. Li, C. C. Li, J. C. H. Fung, and X. Q. Lao, 2018: High-resolution satellite remote sensing of provincial $PM_{2.5}$ trends in China from 2001 to 2015. *Atmos. Environ.*, **180**, 110–116, https://doi.org/10.1016/j.atmosenv.2018.02.045.

Lin, M., and Coauthors, 2020: Vegetation feedbacks during drought exacerbate ozone air pollution extremes in Europe. *Nat. Climate Change*, **10**, 444–451, https://doi.org/10.1038/s41558-020-0743-y.

Lipsey, M. W., and D. B. Wilson, 2001: *Practical Meta-Analysis.* SAGE Publications, 247 pp.

Liu, H., J. Liao, D. Yang, X. Du, P. Hu, Y. Yang, and B. Li, 2014: The response of human thermal perception and skin temperature to step-change transient thermal environments. *Build. Environ.*, **73**, 232–238, https://doi.org/10.1016/j.buildenv.2013.12.007.

——, and Coauthors, 2018: Ground-level ozone pollution and its health impacts in China. *Atmos. Environ.*, **173**, 223–230, https://doi.org/10.1016/j.atmosenv.2017.11.014.

Liu, Y., and T. Wang, 2020: Worsening urban ozone pollution in China from 2013 to 2017—Part 1: The complex and varying roles of meteorology. *Atmos. Chem. Phys.*, **20**, 6305–6321, https://doi.org/10.5194/acp-20-6305-2020.

Logan, J. A., 1985: Tropospheric ozone: Seasonal behavior, trends, and anthropogenic influence. *J. Geophys. Res.*, **90**, 10 463–10 482, https://doi.org/10.1029/JD090iD06p10463.

Lu, X., and Coauthors, 2018: Severe surface ozone pollution in China: A global perspective. *Environ. Sci. Technol. Lett.*, **5**, 487–494, https://doi.org/10.1021/acs.estlett.8b00366.

——, L. Zhang, and L. Shen, 2019: Meteorology and climate influences on tropospheric ozone: A review of natural sources, chemistry, and transport patterns. *Curr. Pollut. Rep.*, **5**, 238–260, https://doi.org/10.1007/s40726-019-00118-3.

——, and Coauthors, 2020: Rapid increases in warm-season surface ozone and resulting health impact in China since 2013. *Environ. Sci. Technol. Lett.*, **7**, 240–247, https://doi.org/10.1021/acs.estlett.0c00171.

Ma, X., H. Jia, T. Sha, J. An, and R. Tian, 2019: Spatial and seasonal characteristics of particulate matter and gaseous pollution in China: Implications for control policy. *Environ. Pollut.*, **248**, 421–428, https://doi.org/10.1016/j.envpol.2019.02.038.

Meehl, G. A., and C. Tebaldi, 2004: More intense, more frequent, and longer lasting heat waves in the 21st century. *Science*, **305**, 994–997, https://doi.org/10.1126/science.1098704.

Mickley, L. J., D. J. Jacob, B. Field, and D. Rind, 2004: Effects of future climate change on regional air pollution episodes in the United States. *Geophys. Res. Lett.*, **31**, L24103, https://doi.org/10.1029/2004GL021216.

Mora, C., and Coauthors, 2017: Global risk of deadly heat. *Nat. Climate Change*, **7**, 501–506, https://doi.org/10.1038/nclimate3322.

Nabizadeh, E., P. Hassanzadeh, D. Yang, and E. A. Barnes, 2019: Size of the atmospheric blocking events: Scaling law and response to climate change. *Geophys. Res. Lett.*, **46**, 13 488–13 499, https://doi.org/10.1029/2019GL084863.

Otero, N., O. Jurado, T. Butler, and H. W. Rust, 2022: The impact of atmospheric blocking on the compounding effect of ozone pollution and temperature: A copula-based approach. *Atmos. Chem. Phys.*, **22**, 1905–1919, https://doi.org/10.5194/acp-22-1905-2022.

Pu, X., T. J. Wang, X. Huang, D. Melas, P. Zanis, D. K. Papanastasiou, and A. Poupkou, 2017: Enhanced surface ozone during the heat wave of 2013 in Yangtze River delta region, China. *Sci. Total Environ.*, **603–604**, 807–816, https://doi.org/10.1016/j.scitotenv.2017.03.056.

Pyrgou, A., P. Hadjinicolaou, and M. Santamouris, 2018: Enhanced near-surface ozone under heatwave conditions in a Mediterranean island. *Sci. Rep.*, **8**, 9191, https://doi.org/10.1038/s41598-018-27590-z.

Qu, Y., J. An, J. Li, Y. Chen, Y. Li, X. Liu, and M. Hu, 2014: Effects of NO_x and VOCs from five emission sources on summer surface O_3 over the Beijing-Tianjin-Hebei region. *Adv. Atmos. Sci.*, **31**, 787–800, https://doi.org/10.1007/s00376-013-3132-x.

Ren, C., G. M. Williams, L. Morawska, K. Mengersen, and S. Tong, 2008: Ozone modifies associations between temperature and cardiovascular mortality: Analysis of the NMMAPS data. *Occup. Environ. Med.*, **65**, 255–260, https://doi.org/10.1136/oem.2007.033878.

Rieder, H. E., A. M. Fiore, L. W. Horowitz, and V. Naik, 2015: Projecting policy-relevant metrics for high summertime ozone pollution events over the eastern United States due to climate and emission changes during the 21st century. *J. Geophys. Res. Atmos.*, **120**, 784–800, https://doi.org/10.1002/2014JD022303.

Rossati, A., 2017: Global warming and its health impact. *Int. J. Occup. Environ. Med.*, **8**, 7–20, https://doi.org/10.15171/ijoem.2017.963.

Russo, S., J. Sillmann, and A. Sterl, 2017: Humid heat waves at different warming levels. *Sci. Rep.*, **7**, 7477, https://doi.org/10.1038/s41598-017-07536-7.

Sánchez-Meca, J., and F. Marín-Martínez, 2010: Meta analysis. *International Encyclopedia of Education*, 3rd ed. P. Peterson, E. Baker, and B. McGaw, Eds., Elsevier, 274–282.

Sanderson, M. G., D. L. Hemming, and R. A. Betts, 2011: Regional temperature and precipitation changes under high-end (≥4°C) global warming. *Philos. Trans. Roy. Soc.*, **369A**, 85–98, https://doi.org/10.1098/rsta.2010.0283.

Schär, C., 2016: The worst heat waves to come. *Nat. Climate Change*, **6**, 128–129, https://doi.org/10.1038/nclimate2864.

Schnell, J. L., and M. J. Prather, 2017: Co-occurrence of extremes in surface ozone, particulate matter, and temperature over eastern North America. *Proc. Natl. Acad. Sci.*, **114**, 2854–2859, https://doi.org/10.1073/pnas.1614453114.

——, and Coauthors, 2016: Effect of climate change on surface ozone over North America, Europe, and East Asia. *Geophys. Res. Lett.*, **43**, 3509–3518, https://doi.org/10.1002/2016GL068060.

Shao, M., Y. Zhang, L. Zeng, X. Tang, J. Zhang, L. Zhong, and B. Wang, 2009: Ground-level ozone in the Pearl River delta and the roles of VOC and NO_x in its production. *J. Environ. Manage.*, **90**, 512–518, https://doi.org/10.1016/j.jenvman.2007.12.008.

Sherwood, S. C., 2018: How important is humidity in heat stress? *J. Geophys. Res. Atmos.*, **123**, 11 808–11 810, https://doi.org/10.1029/2018JD028969.

Stafoggia, M., J. Schwartz, F. Forastiere, and C. Perucci, 2008: Does temperature modify the association between air pollution and mortality? A multicity case-crossover analysis in Italy. *Amer. J. Epidemiol.*, **167**, 1476–1485, https://doi.org/10.1093/aje/kwn074.

Stott, P. A., D. A. Stone, and M. R. Allen, 2004: Human contribution to the European heatwave of 2003. *Nature*, **432**, 610–614, https://doi.org/10.1038/nature03089.

Stull, R., 2011: Wet-bulb temperature from relative humidity and air temperature. *J. Appl. Meteor. Climatol.*, **50**, 2267–2269, https://doi.org/10.1175/JAMC-D-11-0143.1.

Tagaris, E., and Coauthors, 2007: Impacts of global climate change and emissions on regional ozone and fine particulate matter concentrations over the United States. *J. Geophys. Res.*, **112**, D14312, https://doi.org/10.1029/2006JD008262.

Wang, Q., and Coauthors, 2020: Independent and combined effects of heatwaves and $PM_{2.5}$ on preterm birth in Guangzhou, China: A survival analysis. *Environ. Health Perspect.*, **128**, 017006, https://doi.org/10.1289/EHP5117.

Wang, T., L. Xue, P. Brimblecombe, Y. F. Lam, L. Li, and L. Zhang, 2017: Ozone pollution in China: A review of concentrations, meteorological influences,

chemical precursors, and effects. *Sci. Total Environ.*, **575**, 1582–1596, https://doi.org/10.1016/j.scitotenv.2016.10.081.

Wang, Y., and Coauthors, 2020: Contrasting trends of $PM_{2.5}$ and surface-ozone concentrations in China from 2013 to 2017. *Natl. Sci. Rev.*, **7**, 1331–1339, https://doi.org/10.1093/nsr/nwaa032.

Wang, Z., and Coauthors, 2021: Incorrect Asian aerosols affecting the attribution and projection of regional climate change in CMIP6 models. *npj Climate Atmos. Sci.*, **4**, 2, https://doi.org/10.1038/s41612-020-00159-2.

Watts, N., and Coauthors, 2015: Health and climate change: Policy responses to protect public health. *Lancet*, **386**, 1861–1914, https://doi.org/10.1016/S0140-6736(15)60854-6.

Weatherhead, E. C., and Coauthors, 1998: Factors affecting the detection of trends: Statistical considerations and applications to environmental data. *J. Geophys. Res.*, **103**, 17149–17161, https://doi.org/10.1029/98JD00995.

Wei, K., and W. Chen, 2011: An abrupt increase in the summer high temperature extreme days across China in the mid-1990s. *Adv. Atmos. Sci.*, **28**, 1023–1029, https://doi.org/10.1007/s00376-010-0080-6.

WHO, 2020: Air pollution. World Health Organization, www.who.int/health-topics/air-pollution#tab=tab_1.

Willers, S. M., and Coauthors, 2016: High resolution exposure modelling of heat and air pollution and the impact on mortality. *Environ. Int.*, **89–90**, 102–109, https://doi.org/10.1016/j.envint.2016.01.013.

Willett, K. M., and S. Sherwood, 2012: Exceedance of heat index thresholds for 15 regions under a warming climate using the wet-bulb globe temperature. *Int. J. Climatol.*, **32**, 161–177, https://doi.org/10.1002/joc.2257.

Wu, S., L. J. Mickley, E. M. Leibensperger, D. J. Jacob, D. Rind, and D. G. Streets, 2008: Effects of 2000–2050 global change on ozone air quality in the United States. *J. Geophys. Res.*, **113**, D06302, https://doi.org/10.1029/2007JD008917.

Xu, Y., J.-F. Lamarque, and B. M. Sanderson, 2018: The importance of aerosol scenarios in projections of future heat extremes. *Climatic Change*, **146**, 393–406, https://doi.org/10.1007/s10584-015-1565-1.

——, and Coauthors, 2020: Substantial increase in the joint occurrence and human exposure of heatwave and high-PM hazards over South Asia in the mid-21st century. *AGU Adv.*, **1**, e2019AV000103, https://doi.org/10.1029/2019AV000103.

Xue, W., J. Zhang, C. Zhong, D. Ji, and W. Huang, 2020: Satellite-derived spatiotemporal $PM_{2.5}$ concentrations and variations from 2006 to 2017 in China. *Sci. Total Environ.*, **712**, 134577, https://doi.org/10.1016/j.scitotenv.2019.134577.

Zanobetti, A., and A. Peters, 2015: Disentangling interactions between atmospheric pollution and weather. *J. Epidemiol. Community Health*, **69**, 613–615, https://doi.org/10.1136/jech-2014-203939.

Zhang, Q., and Coauthors, 2019: Drivers of improved $PM_{2.5}$ air quality in China from 2013 to 2017. *Proc. Natl. Acad. Sci. USA*, **116**, 24463–24469, https://doi.org/10.1073/pnas.1907956116.

Zhang, Y., P. Yang, Y. Gao, R. L. Leung, and M. L. Bell, 2020: Health and economic impacts of air pollution induced by weather extremes over the continental US. *Environ. Int.*, **143**, 105921, https://doi.org/10.1016/j.envint.2020.105921.

Zhao, B., Y. Su, S. He, M. Zhong, and G. Cui, 2016: Evolution and comparative assessment of ambient air quality standards in China. *J. Integr. Environ. Sci.*, **13**, 85–102, https://doi.org/10.1080/1943815X.2016.1150301.

Zheng, M., L. G. Salmon, J. J. Schauer, L. Zeng, C. Kiang, Y. Zhang, and G. R. Cass, 2005: Seasonal trends in $PM_{2.5}$ source contributions in Beijing, China. *Atmos. Environ.*, **39**, 3967–3976, https://doi.org/10.1016/j.atmosenv.2005.03.036.

Zhu, J., and H. Liao, 2016: Future ozone air quality and radiative forcing over China owing to future changes in emissions under the representative concentration pathways (RCPs). *J. Geophys. Res. Atmos.*, **121**, 1978–2001, https://doi.org/10.1002/2015JD023926.